RESEARCH PAPER

Synthesis and Characterization of $CoFe_2O_4$ and $CuFe_2O_4$ Composited with Hematite by Impregnation Method to Remove Organic Pollutants

Hedayat Gholami[1*], Hassan Koohestani[2] and Mehdi. Ahmadi[3]

** Hedayat.gholami@ut.ac.ir*

Received: February 2020 Revised: June 2020 Accepted: December 2020

[1] School of Metallurgy and Materials Engineering, University College of Engineering, University of Tehran, Tehran, Iran
[2] Faculty of Material and Metallurgical Engineering, Semnan University, Semnan, Iran
[3] Jam Petrochemical Company, Assaluyeh, Boushehr, Iran

DOI: 10.22068/ijmse.18.1.2

Abstract: *In this research, using impregnation method, spinel cobalt and copper ferrites nanoparticles are synthesized on the surface of hematite. Synthesized powders were characterized and examined by FTIR, XRF, XRD, FESEM, BET and EDS analysis and the dye degradation was investigated by UV-vis and AAS methods. Specific surface area increased especially in the sample containing cobalt, which indicates the precise of synthesis and the creation of high surface nanoparticles at hematite surface. The size of particles was in the nano scale and a good uniformity observed in the structure. The results indicated a significant increase in the catalytic ability of hematite nanocomposite. Their catalytic capability investigated by the Fenton reaction with complete removal of methylene blue from the solution via UV-vis irradiation. The samples stability discovered to be excellent by the AAS method.*

Keywords: *Impregnation method, Hematite/$CuFe_2O_4$, Hematite/$CoFe_2O_4$, Spinel ferrites, Fenton reaction.*

1. INTRODUCTION

Spinel ferrites (SFs) are substances with a general formula of MFe_2O_4 in which M is a metal cation (such as Co, Sr, Cu, Ca, Mn, Mg, Fe, Zn and Ni) [1]. In MFe_2O_4 structure, oxygen forms a compact FCC lattice in which M^{+2} and Fe^{+3} ions are located in tetrahedral and octahedral vacant sites respectively. The properties of the ferrites are heavily dependent on the sites, the nature and amount of metal entered into the structure [2]. Their band gap is less than the band gap of catalysts such as WO_3 (2.8 eV), CdS (2.4 eV) and $AgVO_3$ (2.2 eV) which have nano photocatalytic properties under visible light. Example of band gap of some SFs is $CoFe_2O_4$ (2.6 eV), $CoFe_2O_4$ (1.9 eV), $CuFe_2O_4$ (1.32 eV) and $MnFe_2O_4$ (0.98 eV) [3]. Using these photocatalysts with their ability to function in visible zone for the destruction of organic and inorganic pollutants and bacteria has attracted a lot of attention [3, 4].

Magnetic iron oxide, an example of ferrite material has attracted much attention because of its magnetic properties, chemical stability, low toxicity, ease of synthesis and excellent recycling capability, high specific surface and economical cost-effectiveness. They disperse in water very well and can be easily separated by a magnetic field [5, 6].

SFs have a great potential for the removal of pollutant in aqueous solutions, because they have an excellent redox pair based on Fe^{2+}/Fe^{3+} and a conducting solid structure able to disperse electron [7]. Previous researches utilized organic dyes as reactants to evaluate the activities of ferrites. Examples include methyl orange dye, methylene blue solution, Rhodamine B dye, Phenol red and Eosin yellow [3].

Iram et al. [4] synthesized porous hollow magnetic nanoparticles by hydrothermal method and studied its effect on removing the neutral red color. The results show that the color removed effectively in short time and the maximum absorption capacity at 60 min is 105 mg/g for 0.05 g of sample absorbent. The mechanism for removing color by this material can be due to the exchange of ions between the surface of iron oxide and toxic ions of the color [7, 8].

Ai et al. [9] were directly synthesized GNS/Fe_3O_4 composites with a high absorption capability in a facile one-step solvothermal method and an in-situ reaction of converting $FeCl_3$ to Fe_3O_4, which reduced graphene oxide simultaneously. They reported that the resulting composite has shown a great absorption

capability for absorbing methylene blue (MeB) due to having the features of Fe_3O_4 and grapheme [9-11]. According to reports, fast absorption rate of MeB and its removal from water is due to the electrostatic gravity between the negative surface of groups containing oxygen and the positive charge of cationic color (such as MeB) and also the interactions between MeB molecules and aromatic ring [9].

Iron spinel's have good magnetic properties so that in order to separate the nanocomposite by applying an external magnetic field (magnet), the majority of catalyst can be removed [9, 12, 13]. The researchers have investigated the possibility of adding hematite on the surface of ferrite nanoparticles. Remarkably, the main function of hematite in MFe_2O_4 is to controlled catalytic, optical and magnetic properties [6].

In this study, $CoFe_2O_4$ and $NiFe_2O_4$ spinels were synthesized and then were precipitated on hematite particle surface. The hematite used is obtained from the slag of the steelmaking process. In fact, it allows for the recovery of steel slag, which has never been the investigation before. The produced composites were investigated using XRD, FESEM, FTIR and BET. Catalytic activity of samples was studied by the degradation of methyl blue.

2. EXPERIMENTAL PROCEDURES

2.1. Materials

Copper sulphate ($CuSO_4.5H_2O$), cobalt chloride ($CoCl_2.6H_2O$), hydrogen peroxide 30% (H_2O_2), methylene blue ($C_{16}H_{18}ClN_3S$), sodium hydroxide (NaOH) and hydrochloric acid (HCl) were purchased from Merck. All other reagents were of analytical grade.

2.2. Synthesis Method

The base material in this work was hematite, and spinel cobalt ferrite and spinel copper ferrite nanoparticles were synthesized on its surface. The impregnation method was used for synthesis. Initially, some specified hematite (powder) was added to the deionized water and then was stirred at high speed to become completely smooth and distributed. After preparing the mixed solution, its pH was adjusted to initiate the reaction. Sodium hydroxide and hydrochloric acid were used to set the pH in the range of 7 to 8.

The desired amount of copper and cobalt compounds were dissolved in a certain amount of water and after that, hematite solution was added to the stirring suspension drop by drop. After two hours, nanoparticles formed on the surface of hematite. Finally, the resulting suspension was dried while stirring at 100°C on a heater. The calculations were made so that catalysts contained 5 wt.% of the desired metals, and two composites hematite/$CoFe_2O_4$ (HCo) and hematite/$CuFe_2O_4$ (HCu) were obtained.

2.3. Characterization

The elemental analysis and the amount of elements present in the samples were determined by x-ray fluorescence (XRF, ADVANT, USA) analysis. X-ray diffraction (XRD, Phillips PW 3710, The Netherlands) with CuKα radiation=1.5405Å was used to identify the phases. The morphology and particles size of the produced composites were investigated by a field-emission scanning electron microscope (FESEM, TESCAN- MIRA2, Czech Republic). To examine the desired hematite chemical analysis, a test was performed by energy-dispersive x-ray spectroscopy technique (EDS). The specific surface area of samples was obtained using BET (Belsorp mini II, Japan). FT-IR spectra of the composites were obtained by using a Perkin Elmer 400 spectrometer (Bruker Optic) in the range of 400-4000 cm^{-1}.

To investigate the catalytic performance of produced composites, Fenton reaction for methyl blue was used. 1000 ml aqueous solution of methyl orange (initial concentration, 100 mg/l) was stirred at 250 rpm into a cylindrical glass vessel. Produced composites (100 mg) and 2 ml of hydrogen peroxide were then added into the solution at room temperature. After 60 min, the MeO concentration was determined using UV-Vis spectrophotometer (Jenway-6705) at the maximum absorption wavelength (664 nm).

3. RESULTS AND DISCUSSION

3.1. XRD

Figure 1 show the XRD patterns of hematite and produced composites. As shown in Figure 1a, the main phase is the hematite with a high compliance rate with additional specifications (JCPDS No. 01-080-2377). However, some changes occurred after synthesis of composites due to the presence of new phases and bonding with the combined metallic materials along with

hematite. The absence of any phase based on the presence of pure cobalt and copper shows that most of these metals added to catalyst reacted with hematite and turned into spinel ferrites. Therefore, hematite in the $CoFe_2O_4$ and $CuFe_2O_4$ samples was identified with JCPDS No. 01-089-2810 and JCPDS No. 01-079-0007, respectively. According to Figure 1b and JCPDS No. 00-003-0864 related to spinel phase $CoFe_2O_4$, the combination of cobalt with iron in catalyst is confirmed. Also, based on Figure 1c, and JCPDS No. 00-034-0425, copper was added to the structure of hematite and created a new compound known as the spinel phase $CuFe_2O_4$. Also changing the reference number card of pure hematite from JCPDS No. 01-080-2377 to JCPDS No. 01-079-0007 in combination mode indicates the phase change after the introduction of copper into hematite. Yen et al. synthesized the mesoporous bimetal oxides of $CuFe_2O_4$ by impregnation method and by investigating the X-results showed that $CuFe_2O_4$ composition is pure and did not observe any additional peaks in the XRD pattern [14].

3.2. XRF

After the synthesis process, the sample containing 5 wt.% of copper and cobalt was examined by XRF method in order to ensure to the accuracy of the test and the method of calculating the values. The results are presented in Table 1. As can be seen, the percentage of copper and cobalt in the sample is 4.9% and 4.93%, respectively which indicates the precision of the synthesis process and accuracy of the basis for the batch calculation.

3.3. FESEM

FESEM images of samples are shown in Figure 2. By investigating of the images, in spinel Co and Cu ferrites, nanoparticles with a size below 35 nm on the hematite surface can be identified. After observing the FESEM image of hematite (Figure 2a), it can be said that the average particle size ranged from micron to nano dimensions. The morphology of most particles was spherical. Nanoparticles containing copper and cobalt (Figures 2b and 2c) in sizes below 35 nm with spherical shapes were observed on the surface of hematite, which in some way indicates the optimal synthesis of these catalysts. Li et al. synthesized $CuFe_2O_4$ nanoparticles with a size of 10 nm and an almost spherical morphology by impregnation method [15].

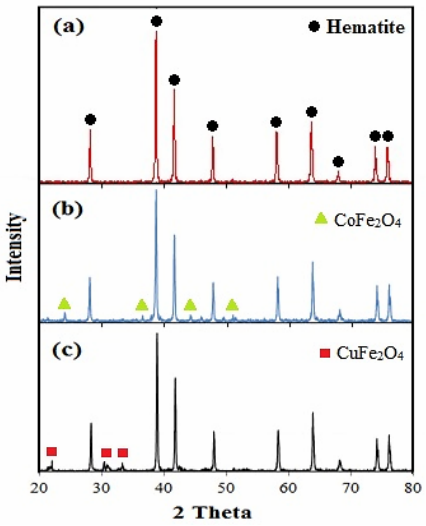

Fig. 1. XRD patterns of a) hematite, b) $CoFe_2O_4$/hematite and c) $CuFe_2O_4$/hematite samples.

Table 1. XRF result of HCu and HCo samples containing 5wt.% Cu and Co.

wt%	Mn	Na	Fe	Si	Cu	Co	Cl	Ca	Al	Mg	S
HCu	0.126	0.37	58.36	0.42	4.9	0	0.6	0.357	0.158	0.12	2
HCo	0.97	0.12	56.02	0.51	0	4.93	1.2	0.21	0.321	0.034	1.2

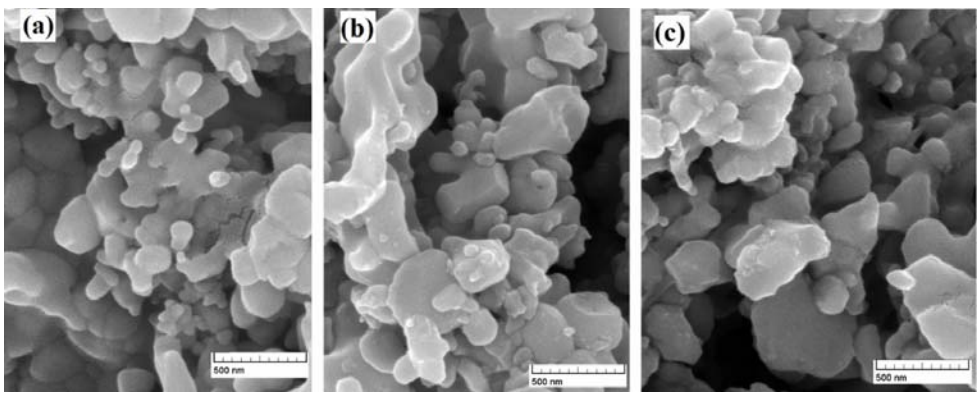

Fig. 2. FESEM images of a) hematite, b) hematite/$CoFe_2O_4$ and c) hematite/$CuFe_2O_4$ samples.

Energy-dispersive x-ray spectroscopy (EDS) of samples is shown in Figure 3. Based on Figure 3a, the amount of iron and oxygen in hematite are 70.25% and 29.75% respectively, confirming the purity of hematite. The results and patterns of EDS related to synthesized composites are shown in Figures 3b and 3c. It verifies the elements which are loaded on hematite in nano catalysts. Peaks of cobalt and copper elements are shown in Figures 3b and 3c. Given that during the synthesis of catalysts, the desired amount of each metal was considered 5 wt%, after conducting EDS, the average percentage of cobalt and copper elements was 4.96 wt.% which shows the accuracy of the synthesis process and calculations.

3.4. Specific Surface Area (by BET)

Based on the results of BET analysis, the specific surface area of hematite was calculated 3.598 m^2/g. The BET chart of hematite is shown in Figure 4. Surface areas of HCo and HCu were 20.619 and 4.0886 m^2/g, also pore diameter of HCo and HCu are 13.395 and 62.481 nm, respectively. As the surface area increases, the number of active sites for catalytic reaction and the catalytic reaction rate increases as well.

The surface area of HCo composite is more than pure hematite and HCu samples, which is a special privilege. Some of the factors that increase the specific surface area in synthetic samples include: precise synthesis, the addition of Co and Cu particles in the hematite structure, the formation of spinel ferrite nanoparticles with very high surface area, preventing the agglomeration of particles with temperature control and continuous stirring of solution during the synthesis. Figure 5 shows N_2 adsorption-desorption isotherms of HCo and HCu.

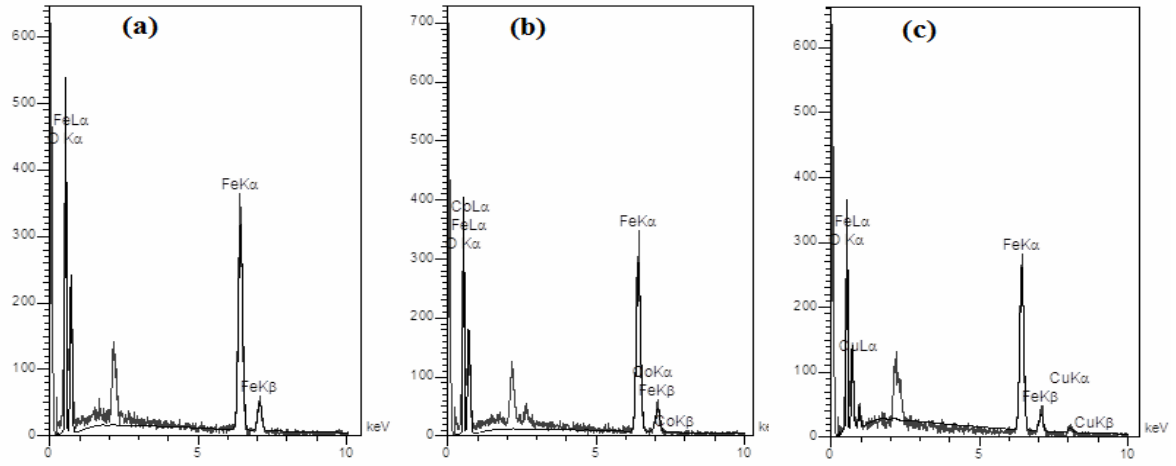

Fig. 3. X-ray diffraction spectroscopy (EDS) result of a) hematite, b) hematite/$CoFe_2O_4$ and c) hematite/$CuFe_2O_4$ samples.

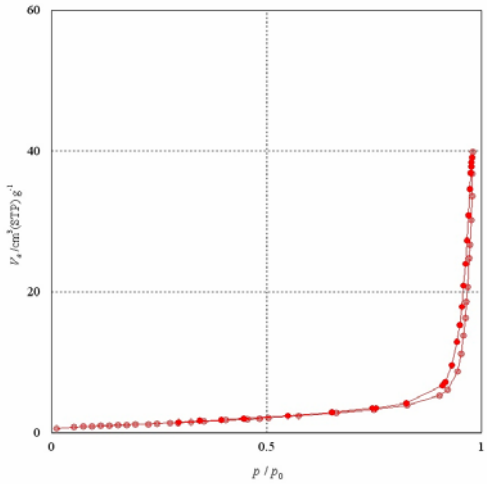

Fig. 4. N_2 adsorption-desorption isotherms of Hematite.

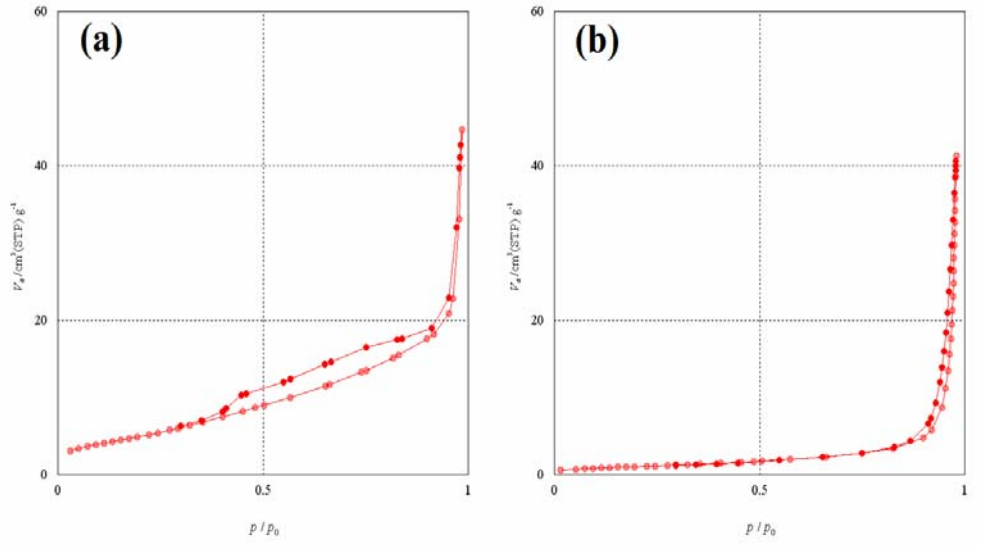

Fig. 5. N_2 adsorption-desorption isotherms of a) HCo and b) HCu composites.

3.5. Fourier-Transform Infrared Spectroscopy (FTIR)

FTIR analysis was performed on the synthesized samples in order to ensure the presence of spinel ferrite compounds and also to prove the absence of other phases in the compound. In Figure 6, the result of FTIR regarding HCo and HCu can be seen.

As can be seen, most peaks in the two samples have a similar wave number but with different passing percentage. This can indicate the existence of links with a high degree of similarity in both samples. The Ferrite can be introduced as continuous crystals by bonding through ionic, covalent or vander Walls forces to the nearest neighbors. In ferrite, the metal ions are located in two different sub-lattices, namely tetrahedral (sites A) and octagonal (sites B), according to the geometric arrangement of the oxygen neighbors of the nearest neighbors [16]. Two main broad metal-oxygen bands ν1 and ν2 at 530-590 and 450-480 cm^{-1} can be seen. ν1, the highest one, corresponds to intrinsic stretching vibrations of tetrahedral metal-oxygen bonding (sites A), whereas ν2 is assigned to octahedral metal stretching (sites B) [17]. It is known that Co^{2+}, Cu^{2+} and Fe^{3+} ions can occupy both octahedral and tetrahedral sites. With the help of this method, the presence of spinel cobalt and copper ferrites were identified by XRD method, which was proved again. Other researchers have reported similar peaks in the FTIR spectrum [14, 16, 18].

3.6. Catalytic Activity of Synthesized Composites

In this test, methylene blue (MeB) degradation in the presence of hematite and two synthesized composites as catalysts by Fenton reaction was investigated. At first, the effect of hydrogen peroxide on MeB degradation was studied (Table 2). Two sample solutions were selected; the first one dye degradation examined without the Fenton reaction and the second one investigated the dye absorption after contact with hematite under Fenton reaction. The test time was considered one hour. In fact, in second solution, both catalyst (hematite) and hydrogen peroxide were added, while in the other solution only the catalyst was studied without hydrogen peroxide.

The results show that under Fenton reaction a significant effect on the performance of the hematite catalyst had happened. As of 6.6% in the presence of hematite only, it reached 77.74% in the presence of hematite and H_2O_2. Zero-valent Fe (Fe^0) is an efficient catalyst in the heterogeneous Fenton-like reaction in water treatment due to the production of ferrous iron by the corrosion of metal iron. Furthermore, Fe^0 act as an electrons donor and reduce Fe^{3+} to Fe^{2+}, which could be able to accelerate the formation of $^{\bullet}OH$ [19].

After initial examination, the activity of HCo and HCu catalysts were tested for Fenton reaction. In order to increase the accuracy and the possibility of a more accurate comparison, the conditions and methods of testing, the test conditions and procedure were the same as the

previous one, but with a catalyst amount of 10 mg each. Then, the absorption rate of ultraviolet radiation was measured for these three solutions and their concentrations were calculated. The results of MeB concentration determination by UV-vis spectrophotometer are presented in Table 2. Macro images of the MeB color change are also shown in Figure 7.

Figure 8a shows the percentage of decolorization by synthesized composites. As can be seen at low times, the ability of HCo to remove dye is higher than HCu, but at long times the ability of the two will be closer. Zhang et al. showed that $CoFe_2O_4$ alone can remove only 6.6% of rhodamine B after 45 min in UV-vis light [20]. Shahid et al synthesized $MgFe_2O_4$ photocatalyst and showed photodegradation rate of $MgFe_2O_4$ was 95% of the Methylene blue molecules for 50 min [21]. In a study, Cheng et al. demonstrated in the presence of $CuFe_2O_4$ photocatalyst, the photocatalytic Fenton degradation of glycerol improved substantially to record nearly 40.0 % degradation after 250 min at a catalyst loading of 5.0 g/L [22]. Many researchers have shown in their work that the removal of methylene blue by the reaction of Fenton and UV light by catalysts follows pseudo-second-order kinetic model. The pseudo-first-order kinetic equation is expressed as follows [23-25]:

$$\frac{t}{q_t} = \frac{1}{kq_e^2} + (\frac{1}{q_e})t \qquad (1)$$

Where k (g/mg.min), is the rate constant, q_e (mg/g) is the amount of solute adsorbed on the surface at equilibrium and q_t (mg/g) is the amount of solute adsorbed at any time. The pseudo-second-order rate constants and the corresponding linear regression correlation coefficients R^2 are given in Fig 8b. The reaction constants for HCu and HCo are 0.0263 and 0.0325 g/mg.min, respectively.

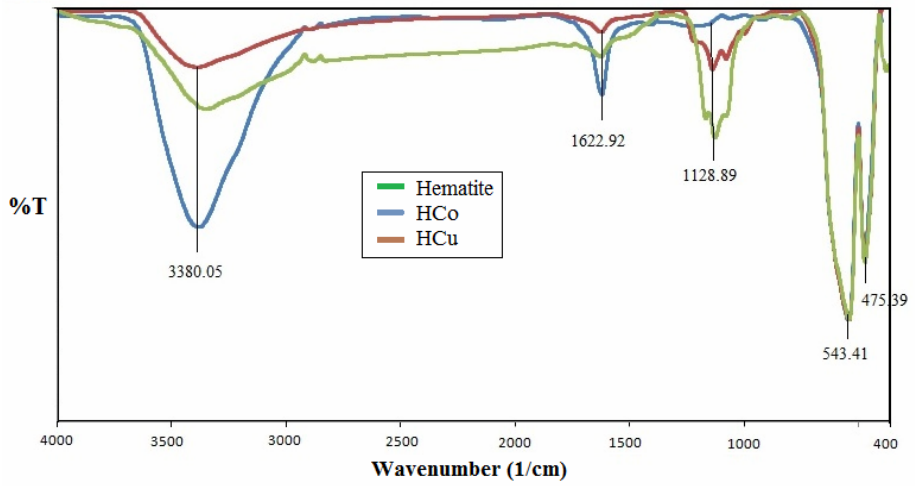

Fig. 6. FTIR patterns of hematite, HCo and HCu.

Table 2. The de-colorization efficiency by different reactants.

	Samples	De-colorization %
1	Standard MeB solution	0
2	Only hematite	6.6
3	Hematite + H_2O_2	77.74
4	HCo + H_2O_2	99.5
5	HCu + H_2O_2	99.65

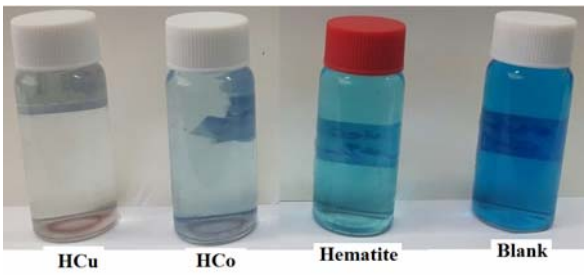

Fig. 7. Images of MeB de-colorization in Fenton reaction by synthesized catalysts.

Copper and cobalt can convert the H_2O_2 to produce active hydroxyl radicals ($^{\bullet}OH$) via a Fenton-like reaction. While the catalytic performance of iron ion, Fe^{2+} is higher at lower pH, Cu and Co ions react to oxidants formation with higher activity at alkaline pH conditions [26]. The very active hydroxyl free radicals are effectively destructed organic pollutants, therefore are used for organic waste treatment in industries [27]. In hematite/$CuFe_2O_4$, the Cu(II)-O-Fe(III) species are catalytically active centers for phenol hydroxylation with H_2O_2 being used as the hydroxylation reagent. The OH radicals were generated via the decomposition of H_2O_2 over Cu(II)-O-Fe(III) due to the existence of Fe(III) in the catalyst through the formation of the Fenton-like reaction [28, 29].

Stability of catalyst is one of the most important factors in the field of heterogeneous catalysts and especially industrial catalysts [30-32]. Stability is not a concern for homogeneous catalysts because of the impossibility of recycling homogeneous catalysts.

Reusability of HCu and HCo catalysts with conditions similar to previous Fenton reaction tests was investigated. Degradation of MeB solution with a concentration of 100 mg/l was performed with catalysts during five sequential Fenton tests. At the end, repeated testing did not show any significant changes or deviations, and degradation did not reach below 97.5% in copper catalyst and 92% in catalyst containing cobalt (Figure 9).

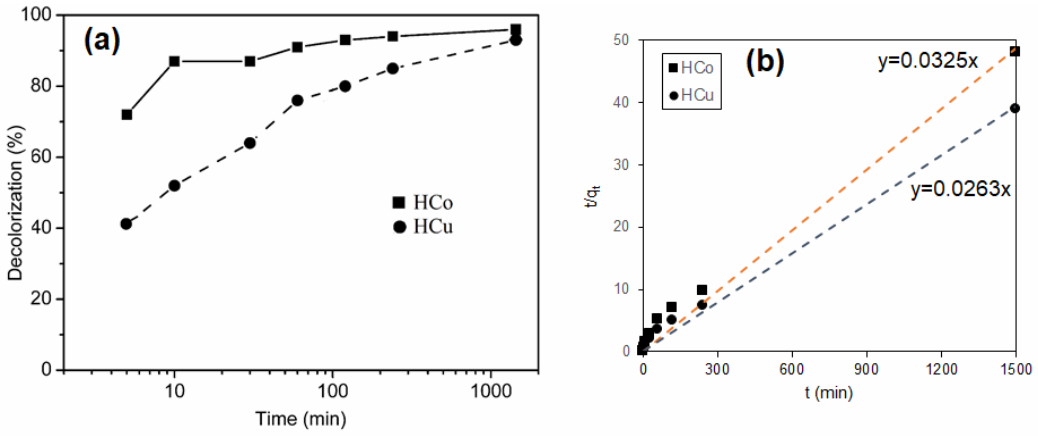

Fig. 8. a) Catalytic ability and b) Pseudo-second-order kinetics for degradation of MeB.

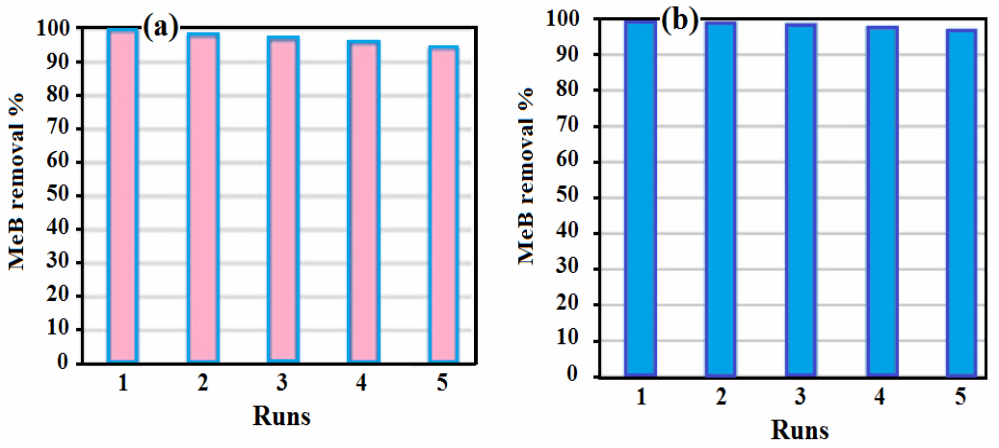

Fig. 9. Reusability of composites containing a) copper and b) cobalt.

4. CONCLUSION

The synthesis of spinel copper and cobalt ferrite nanoparticles on hematite surface were carried out. With the addition of copper and cobalt, significant increase in the catalytic ability of hematite was observed. The results showed that nano structures with spherical and uniform morphology formed on hematite particles surface. It was also found that the synthesized catalysts have good stability and can be reused.

REFERENCES

1. Schwartz, J. and Kittel, T., Ferrite thick films and chemical solution-based methods of preparation thereof. 2017, Google Patents.
2. Mathew, D. S. and Juang, R.-S., "An overview of the structure and magnetism of spinel ferrite nanoparticles and their synthesis in microemulsions", Chem. Eng. J., 2007, 129(1-3), 51-65.
3. Casbeer, E., Sharma, V. K. and Li, X.-Z., "Synthesis and photocatalytic activity of ferrites under visible light: a review", Sep. Purif. Technol., 2012, 87, 1-14.
4. Iram, M., Guo, C., Guan, Y., Ishfaq, A., Liu, H., "Adsorption and magnetic removal of neutral red dye from aqueous solution using Fe_3O_4 hollow nanospheres", J. Hazard. Mater., 2010, 181(1-3), 1039-1050.
5. Santhosh, C., Kollu, P., Doshi, S., Sharm, M., Bahadur, D., Vanchinathan, M. T., Saravanan, P., Kime, B.-S. and Grace, A. N., "Adsorption, photodegradation and antibacterial study of graphene-Fe_3O_4 nanocomposite for multipurpose water purification application", Rsc Advances, 2014, 4(54), 28300-28308.
6. Zhu, N., Ji, H., Yu, P., Niu, P., Farooq, M. U., Akram, M. W., Udego, I. O., Li, H. and Niu, X., "Surface modification of magnetic iron oxide nanoparticles", Nanomater., 2018, 8(10), 810.
7. Al Yaqoob, K., Bououdina, M., Akhter, M.S., Al Najar, B. and Vijaya, J. J., "Selectivity and efficient Pb and Cd ions removal by magnetic MFe_2O_4 (M= Co, Ni, Cu and Zn) nanoparticles", Mater. Chem. Phys., 2019, 232, 254-264.
8. Zhong, L.S., Hu, J.-S., Liang, H.-P., Cao, A.-M., Song W.-G. and Wan, L.-J., "Self-Assembled 3D flowerlike iron oxide nanostructures and their application in water treatment", Adv. Mater., 2006, 18(18), 2426-2431.
9. Ai, L., Zhang, C. and Chen, Z., "Removal of methylene blue from aqueous solution by a solvothermal-synthesized graphene/magnetite composite", J. Hazard. Mater., 2011, 192(3), 1515-1524..
10. Vinothkannan, M., Karthikeyan, C., Kumar, G. G., Kim, A. R. and Yoo, D. J., "One-pot green synthesis of reduced graphene oxide (RGO)/Fe_3O_4 nanocomposites and its catalytic activity toward methylene blue dye degradation", Spectrochim. Acta, Part A, 2015, 136, 256-264.
11. Koohestani, H. "Synthesis and characterisation of TiO_2 nanoparticles/Fe_2O_3 waste chips composite", Micro Nano Lett., 2019, 14, 678-682.
12. Wang, C., Feng, C. Gao, Y., Ma, X., Wu, Q. and Wang, Z., "Preparation of a graphene-based magnetic nanocomposite for the removal of an organic dye from aqueous solution", Chem. Eng. J., 2011, 173(1), 92-97.
13. Verma, K., Goyal, N., Singh, M., Singh, M. and Kotnala, R. K., "Hematite α-Fe_2O_3 induced magnetic and electrical behavior of $NiFe_2O_4$ and $CoFe_2O_4$ ferrite nanoparticles", Results in Phys., 2019, 13, 102212.
14. Yen, H., Seo, Y., Guillet-Nicolas, R., Kaliaguine, S. and Kleitz, F., "One-step-impregnation hard templating synthesis of high-surface-area nanostructured mixed metal oxides ($NiFe_2O_4$, $CuFe_2O_4$ and Cu/CeO_2)", Chem. Commun., 2011, 47(37), 10473-10475.
15. Li, B., Li, M., Yao, C., Shi, Y., Ye, D., Wu, J. and Zhao, D., "A facile strategy for the preparation of well-dispersed bimetal oxide $CuFe_2O_4$ nanoparticles supported on mesoporous silica", J. Mater. Chem. A, 2013, 1(23), 6742-6749.
16. Selvan, R. K., Augustin, C. O., Berchmans, L. and Saraswathi, R., "Combustion synthesis of $CuFe_2O_4$", Mater. Res. Bull., 2003, 38(1), 41-54.
17. Senthil, V., Gajendiran, J., Raj, S. G., Shanmugavel, T., Kumar, G. R. and Reddy, C. P., "Study of structural and magnetic properties of cobalt ferrite ($CoFe_2O_4$) nanostructures", Chem. Phys. Lett., 2018, 695, 19-23.

18. Karim, K.M.R., Karim, R., Tarek, M., Sarkar, S. M., Mouras, R., Ong, H. R., Abdullah, H., Cheng, C. K. and Khan, M. M. R., "Photoelectrocatalytic reduction of CO_2 to methanol over $CuFe_2O_4$@ PANI photoathode", Int. J. Hydrogen Energy, 2020, DOI: 10.1016/j.ijhydene.2020.02.195
19. Qin, Q., Liu, Y., Sun, T. and Xu, Y., "Enhanced heterogeneous Fenton-like degradation of methylene blue by reduced $CuFe_2O_4$", RSC Advances, 2018, 8(2), 1071-1077.
20. Zhang, H., Nengzi, L., Liu, Y., Gao, Y. and Cheng, X., "Efficient removal of organic pollutant by activation of persulfate with magnetic $Co_3O_4/CoFe_2O_4$ composite", Arabian J. Chem., 2020, 13(5), 5332-5344.
21. Shahid, M., Jingling, L., Ali, Z., Shakir, I., Warsi, M. F., Parveen, R. and Nadeem, M., "Photocatalytic degradation of methylene blue on magnetically separable $MgFe_2O_4$ under visible light irradiation", Mater. Chem. Phys., 2013, 139(2-3), 566-571.
22. Cheng, C.K., Kong, Z.Y. and Khan, M.R., "Photocatalytic-Fenton Degradation of Glycerol Solution over Visible Light-Responsive $CuFe_2O_4$", Water, Air, Soil Pollut., 2015, 226(10), 327.
23. Hameed, B., Krishni, R. and Sata, S., "A novel agricultural waste adsorbent for the removal of cationic dye from aqueous solutions", J. Haz. Mater., 2009, 162(1), 305-311.
24. Wu, Y., Zeng, S., Wang, F., Megharaj, M., Naidu, R. and Chen, Z., "Heterogeneous Fenton-like oxidation of malachite green by iron-based nanoparticles synthesized by tea extract as a catalyst", Sep. Purif. Technol., 2015, 154, 161-167.
25. Yang, B., Tian, Z., Zhang, L., Guo, Y. and Yan, S., "Enhanced heterogeneous Fenton degradation of Methylene Blue by nanoscale zero valent iron (nZVI) assembled on magnetic Fe_3O_4/reduced graphene oxide", J. Water Proc. Eng., 2015, 5, 101-111.
26. Pillai, K.C., Kwon, T. O. and Moon, I. S., "Degradation of wastewater from terephthalic acid manufacturing process by ozonation catalyzed with Fe^{2+}, H_2O_2 and UV light: Direct versus indirect ozonation reactions", Appl. Catal., B, 2009, 91(1-2), 319-328.
27. Ren, Y., Lin, L., Ma, J., Yang, J., Feng, J. and Fan, Z., "Sulfate radicals induced from peroxymonosulfate by magnetic ferrospinel MFe_2O_4 (M= Co, Cu, Mn and Zn) as heterogeneous catalysts in the water", Appl. Catal., B, 2015, 165, 572-578.
28. Zhao, Y., He, G., Dai, W. and Chen, H., "High catalytic activity in the phenol hydroxylation of magnetically separable $CuFe_2O_4$-reduced graphene oxide", Ind. Eng. Chem. Res., 2014, 53(32), 12566-12574.
29. Feng, Y., Lee, P. H., Wu, D., Zhou, Z., Li, H. and Shih, K., "Degradation of contaminants by Cu^{+}-activated molecular oxygen in aqueous solutions: Evidence for cupryl species (Cu^{3+})", J. Haz. Mate., 2017, 331, 81-87.
30. Munoz, M., de Pedro, Z. M., Casas, J. A. and Rodriguez, J. J., "Preparation of magnetite-based catalysts and their application in heterogeneous Fenton oxidation-a review", Appl. Catal., B, 2015, 176, 249-265.
31. Sharma, S. K., Green chemistry for dyes removal from waste water: research trends and applications, 2015, Wiley-Scrivener, 1-34..
32. Nidheesh, P., "Heterogeneous Fenton catalysts for the abatement of organic pollutants from aqueous solution: a review", Rsc Advances, 2015, 5(51), 40552-40577.